Chapter 12
A New Experiment and Modelling Work to Jointly Identify the Building Envelope's Thermal Parameters and a Physical Solar Aperture

Guillaume Lethé

Abstract Co-heating tests have been used by many researchers for the characterisation of the heat loss coefficient (HLC) of building envelopes. Measurements may be analysed through static, transient or dynamic approaches. A reliable identification of the HLC is obtained by the joint identification of multiple parameters including the solar aperture. The solar gains continuously depend on the relative position of the sun with regard to the building's glazed components and on the type of emitted radiation, ranging from diffuse (overcast sky) to beam (clear sky). However in state-of-the-art static co-heating tests, only the daily mean solar radiation is analysed, leading to the identification of a static solar aperture (A_w). Practitioners then have to rely on several weeks of continuous measurements under representative but not extreme weather conditions to derive regression lines with acceptable correlation coefficients between the daily means of the measured variables. Finally, the obtained results do not allow performing dynamic predictions since the model is static. This paper first explains the advantages of the newly developed experimental protocol itself, compared to other dynamic tests recently applied in situ. It also presents a new methodology to better take the solar gains into account during the dynamic analysis of a short experiment. The proposed methodology jointly enables a more accurate identification of the general heat loss characteristics of the building and of a physically-interpretable and climate-independent solar aperture. It can be seen as the equivalent total solar transmission coefficient of the envelope under normal incidence, multiplied by the total glazed surface of the whole building envelope, and is denoted as $gA_{eq,tot,\perp}$ (replaces A_w). The proposed method can be applied to characterize the static energy

Lethé, G. (2015) **A new experiment and modelling work to jointly identify the building envelope's thermal parameters and a physical solar aperture** *In;* Gorse, C and Dastbaz, M (Eds.) *International SEEDS Conference* ,17–18 September 2015, Leeds Beckett University UK, Sustainable Ecological Engineering Design for Society.

G. Lethé (✉)
Former Belgian Building Research Institute, Brussels, Belgium
e-mail: guillaume.lethe@gmail.com

M. Dastbaz and C. Gorse (eds.), *Sustainable Ecological Engineering Design*,
DOI 10.1007/978-3-319-32646-7_12

performance of the building and also to predict (or even control) the energy consumption under specific weather forecasts or normalized conditions.

Keywords Co-heating test · Control · Dynamic sequence · Grey-box model · On-site measurement · Solar aperture · Solar pre-processor · Thermal performance

Introduction

On-site measurement campaigns and data analysis require in-depth and balanced skills regarding the test environment, the experimental procedure and the data analysis. While the *in situ* measurement and identification of static performance indicators of building components are already covered by a standard (ISO 2014), global building envelopes are still under investigation as exemplified in (Gorse et al. 2014). The Heat Loss Coefficient (HLC in W/K) expresses the heating power that is lost by transmission and exfiltration (under sealed ventilation system) through a building envelope under a temperature gradient of 1 K. Methods to determine a building's thermal dynamics go along with an accurate identification of its response to temperature changes, solar radiation, exfiltration rate and its effective thermal capacity (Bacher and Madsen 2011; Johnston et al. 2013; Pandraud et al. 2013; Bauwens and Roels 2014). The application of a 'hybrid' dynamic thermal solicitation sequence and subsequent data analysis has been investigated, while better taking the solar gains into account thanks to a new methodology developed in this paper.

The short hybrid dynamic thermal solicitation sequence of the building has been presented in (Lethé et al. 2014), was partly been inspired from (Subbarao et al. 1988; Bacher et al. 2010; Bacher 2013; Steskens et al. 2014), and is the baseline for the present paper. This sequence combines characteristics of smoothly assembled segments of quasi-static, pseudo-random binary sequences (PRBS) and multi-sine operation eventually aimed at enforcing optimal decorrelation of the acquired data series used as inputs and output of the dynamic model to be identified. Air change rate was also measured in order to enable us to identify with good reproducibility the specific transmission part of the total heat loss coefficient in various wind conditions and independently of the air exfiltrations. This was necessary for the present case study where the exfiltration heat losses exceeded 15 % of the total heat losses on average, with sealed ventilation system.

Various treatments of the solar radiation measurements, already developed in (Lethé et al. 2013), are used in detail in this study in order to determine what we have called here the equivalent total solar transmission coefficient of the envelope (mainly the glazed components) under normal incidence, $gA_{eq,tot,\perp}$.

Below, we firstly (see Section "Energy Balance of a Building Envelope") write the dynamic energy balance of the building envelope that was used in this study, in conformity with the notations of the EN ISO 13789 standard. We then (see Section "A Rich and Short Hybrid Dynamic Solicitation Sequence") describe the (hybrid) dataset that has been generated and used. The dynamic analysis of the data (see Section "Dynamic Data Analysis") allowed us to compare the results obtained with the state-of-the-art solar model and the newly enhanced one. Finally (see Section "Conclusions") we sketch advantages and drawbacks, opportunities and remaining questions towards better dynamic thermal modelling and performance identification of buildings.

Energy Balance of a Building Envelope

Various modelling, from the very simple towards more complex (static, transient, dynamic), are already developed (Bacher and Madsen 2011; Pandraud et al. 2013; Bauwens and Roels 2014; Subbarao et al. 1988). We briefly expose the dynamic model that has presently been used.

The most promising analysis methods are parameter identification methods applied on well decorrelated dynamic data sets. The following grey-box stochastic model is used to represent the entire building. It is rather simple but often appears suitable:

$$\mathrm{d}T_i = \frac{(T_e - T_i)}{R_{ie}C_i}\mathrm{d}t + \frac{Q_h}{C_i}\mathrm{d}t + \frac{A_w q_s}{C_i}\mathrm{d}t - \frac{Q_V}{C_i}\mathrm{d}t + \sigma_i d\omega_i \tag{12.1}$$

$$\mathrm{d}T_e = \frac{(T_i - T_e)}{R_{ie}C_e}\mathrm{d}t + \frac{(T_a - T_e)}{R_{ea}C_e}\mathrm{d}t + \sigma_e \mathrm{d}\omega_e \tag{12.2}$$

$$\frac{1}{R_{ie} + R_{ea}} \cong HLC - \frac{Q_V}{T_i - T_a} = UA \tag{12.3}$$

where T_i, T_e and T_a are respectively the indoor air, the building envelope and the ambient (outdoor air) temperatures, R_{ie} is the thermal resistance between the interior and the building envelope, R_{ea} is the thermal resistance between the building envelope and the interior thermal medium, C_i and C_e are the heat capacities of the interior (internal walls) and of the building envelope (external walls), Q_h is the energy flux from the heating system, $A_w q_s$ is the solar aperture multiplied by the energy flux density from the solar radiation (further defined in Section "Dynamic Data Analysis"), Q_v is the energy flux from the exfiltrations, ω_i and ω_e are standard Wiener processes, and σ_i and σ_e are the incremental variances of the Wiener processes. The corresponding one-dimensional whole-building equivalent RC-network is presented in Fig. 12.1:

The interior temperature is the output state of the model and is associated with a thermal capacity (air and furniture). The (unobservable) building fabric envelope temperature is assumed to be aggregated in one single node and is obviously associated with a thermal capacity. The overall thermal resistance offered by the

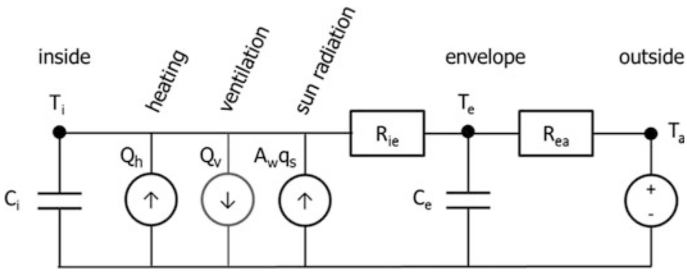

Fig. 12.1 Equivalent RC-network of the whole building envelope thermal model

envelope against the heat losses is represented by two thermal resistances in series. The ambient temperature is chosen as input. Finally, the system is subjected to three other inputs: the electric heating power, the exfiltration losses and the solar radiation, all predominantly acting on the inside air node temperature. The exfiltration loss has been obtained from an instantaneous air change rate measurement using tracer gases at a constant concentration, the instantaneous temperature gradient $T_i - T_a$ and the known volume of the building.

The solar radiation is given in W/m^2 and is associated to an aperture coefficient that gives an equivalent surface through which the radiation is fully transmitted. In this paper, we compare two methodologies to integrate the solar gains. First, the crude global vertical south solar radiation ($q_{s,v,south}$) is used as input, and the parameter A_w is identified. Second, a pre-processed solar radiation, corresponding to the equivalent beam normal incidence total solar radiation ($q_{s,eq,tot,\perp}$), is used as the input and the parameter $gA_{eq,tot,\perp}$ is identified. This second methodology takes into account the relative position of the sun with regard to each glazed component, and the type of radiation received (combination of diffuse and beam radiation).

In order to determine the Heat Loss Coefficient more accurately and detach the individual influence of the solar radiation, the temperature states and the heating power, dynamic data sets and analysis are recommended. Smooth dynamic evolution of the variables of the system, such as the heating power, is preferable to facilitate the statistical validation of the identified model (Lethé et al. 2014), while the temperature homogeneity inside the building has to be guaranteed as much as possible (Johnston et al. 2013). For these reasons an infrastructure that can manage the heating powers of each zone of the building individually and gradually has been used. An optimization analysis scheme (Fig. 12.2) is then applied on the collected data to identify the parameters of the model.

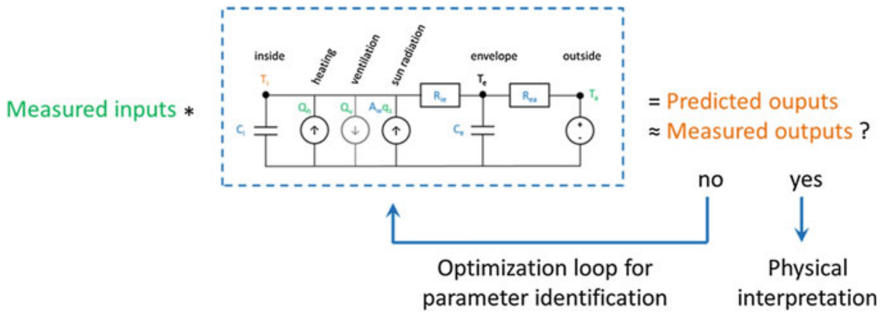

Fig. 12.2 Optimization scheme to identify the parameters of the dynamic model (grey-box model or transfer function) between inputs and outputs

A Rich and Short Hybrid Dynamic Solicitation Sequence

Background Information About the Infrastructure

Dynamic heating sequences have been investigated in order to develop an adapted dynamic co-heating test[1] that more accurately and more robustly identifies the dynamic characteristics of a building envelope model. The optimized developed protocol required individual and continuous sliding control of the injected power (control cycles every 100 s with pulse-width modulation), to ensure smooth data and best temperature homogeneity under all circumstances. The full infrastructure is sketched in Fig. 12.3:

The control and acquisition program has been developed in LabView. In order to ensure best temperature homogeneity when performing power-driven tests, the explicit spread of the total injected power among the zones is obtained with:

$$Q_i^{n+1} = \frac{Q_{tot}^{n+1} Q_i^n / T_i^n}{\sum_i Q_i^n / T_i^n} \tag{12.4}$$

where the Q_i and T_i terms are the zonal powers and temperatures of the preceding cycle and Q_{tot} is the total power required. The superscript $^{n+1}$ stand for the new starting cycle. Additional controls (semi open and closed loop) are included to ensure a robust (no bias) and stable (damped) behaviour of the system. It has been shown (Lethé et al. 2014) that this infrastructure was able to produce smooth transitions and seamless data sets (5 min recording intervals), and to reduce the temperature inhomogeneities by a factor 4 compared to non-adaptive infrastructures using *inter-room* air circulation fans.[2] The comparison means is an indicator expressed as the ratio between the degree-hour difference between the instantaneous hottest ($T_{i,max}$) and coldest ($T_{i,min}$)

[1]The term « co-heating » is not limited here to measurements under constant indoor temperature.

[2]The experiments under investigation are controlled in power and not in temperature.

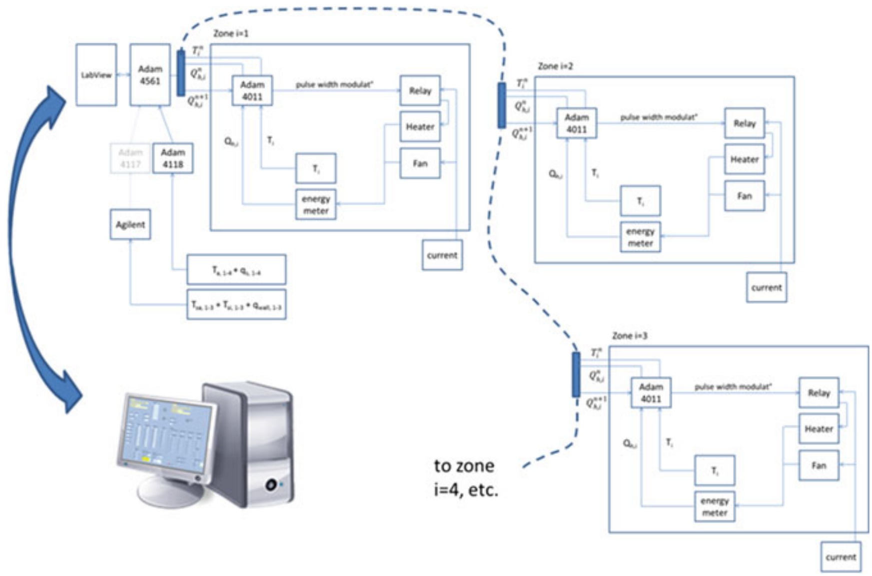

Fig. 12.3 Representation of the infrastructure network. In each zone multi-functional kits are connected to the PC control and acquisition program through a serial port

rooms and the degree-hour difference between the (volume-weighted) average indoor air temperature ($T_{i,mean}$) and ambient air temperature (T_a):

$$\int_{t1}^{t2} \frac{\mathrm{T}_{i,\max}(t) - \mathrm{T}_{i,\min}(t)}{\mathrm{T}_{i,\mathrm{mean}}(t) - \mathrm{T}_{a}(t)} \, \mathrm{d}t \tag{12.5}$$

Note that when temperatures are near-homogeneous, the aggregated indoor air temperature extracted from the volume-weighted average is extremely close to and perhaps even more relevant than the one extracted from a principal component analysis (PCA), which can be sensitive to special conditions and hence not always physically correct.

A Short-Term Hybrid Dynamic Sequence

The developed infrastructure sets the basis for the design of hybrid dynamic heating sequences, exemplified in Fig. 12.4. This sequence is programmatically designed such that the system variables are the least correlated possible and such that the segments are seamlessly connected to avoid harsh residuals in the model output (making the grey-box model validation easier). The entire sequence may last for 4 days if the third day is sunny. It is expected that 5 days are sufficient in most

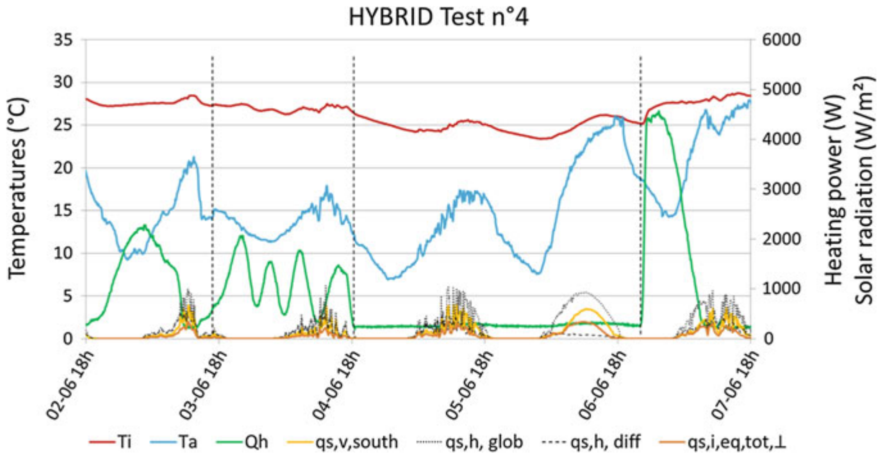

Fig. 12.4 Illustration of the hybrid 4-segments heating sequence

cases if the measurement is planned when the weather forecasts are propitious. More details about this experiment are given in (Lethé et al. 2014).

The infrastructure developed is highly scalable and allows many other types of sequences to be designed. For example, the following function could be used to control the global heating power injected in the building (pure power control):

$$Q_{h,tot} = n \times [sign(\sin(bt^c)) \times abs(\sin(bt^c))^a + d] \quad (12.6)$$

such that the solicitation signal wipes through many frequencies (thanks to the exponent c), related to the typical time constants of interest of the building envelope (thanks to the parameter b) and provides a relatively good signal/noise ratio (thanks to the exponent a and the parameter d). Taking t in hours and the sine function in radians, the parameters a, b, c, d could respectively have the value of 0.25, 3.8, 1.4, and 1.5 (see Fig. 12.5), with n the suited estimated nominal power to achieve a temperature gradient of 10–15 K during the experiment. Other possibilities include an emulation of a residential or tertiary usage of the building, with daily or weekly patterns and a pure thermostatic control.

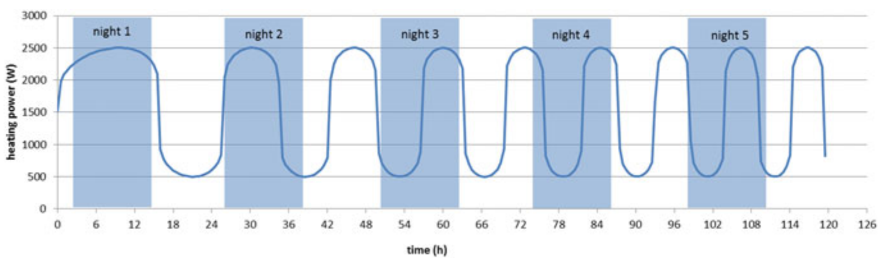

Fig. 12.5 Illustration of the Sine-Sign-Sweep heating sequence

Dynamic Data Analysis

Background on the Test Environment

The detailed test environment description can be found in (Lethé et al. 2014). We here only recall the overall localisation of the equipment inside the house in Fig. 12.6. The ground floor has seven defined zones with the doors widely open. The attic and the basement are disconnected from the ground floor and are each one single volume. The temperature in the attic (not air tight) is highly correlated with the outdoor temperature, such that we consider the 'ceiling-attic-roof' system as a single complex component. The temperature in the basement (faintly ventilated) is quasi-static and close to the outside test-mean temperature (the mean temperature difference between both variables is 1.2 K, i.e. one order of magnitude lower than between the interior and ambient air temperatures). Excluding the basement air temperature to the grey-box model is then found adequate as well. Optimal reproducibility of results under various weather conditions would nevertheless require that the basement temperature be always 'homothetic' to the outdoor and indoor temperatures which is not the case by nature. Results dispersion in function of the temperature conditions in the adjacent spaces is not negligible in general but can be neglected in this particular study. Figure 12.7 presents the four temperature variables discussed here.

Dynamic Analysis of the Data According to Two Methods

In this section, which is the core of the study, we analyse the results obtained following two different methods. The first is the state-of-the-art method where the crude solar data is used as input and the solar aperture is assumed to be a static parameter.

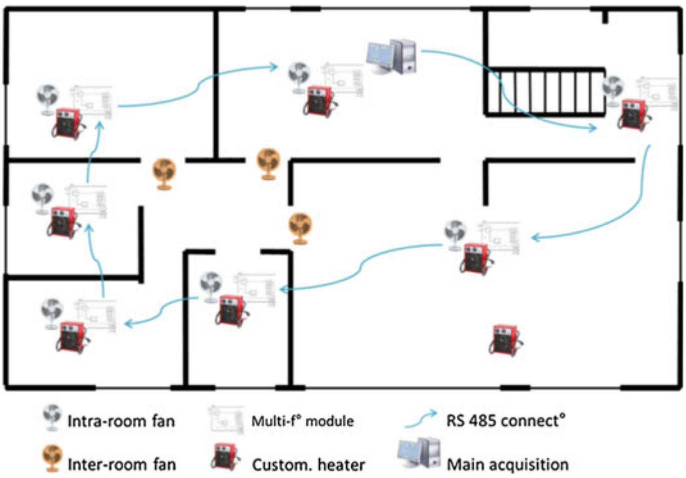

Fig. 12.6 Co-heating infrastructure components and positioning in the house

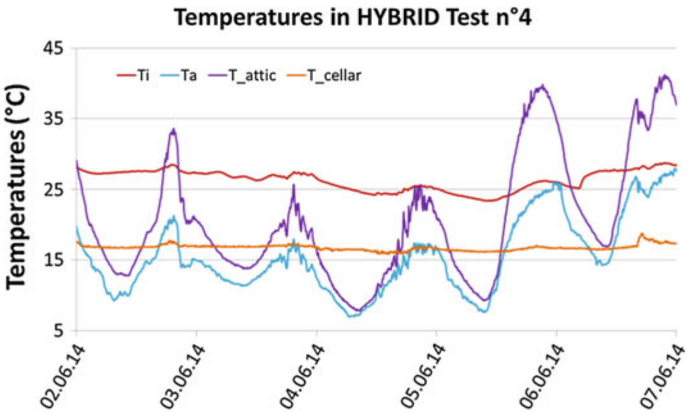

Fig. 12.7 Time series of the main aggregated temperature variables (including attic and cellar)

As explained in the introduction, in a dynamic context, the solar aperture is not a static parameter since the solar gains are not purely proportional to the intensity of the solar radiation. They also depend on the relative angle of the sun with regards to the glazed components on the one side, and on the type of emitted radiation which can range from diffuse (overcast sky) to beam (clear sky). We therefore introduce a more detailed approach.

The newly proposed methodology is expected to produce a more accurate and reliable model identification of the thermal dynamic behaviour of the building (conduction heat losses through the building envelope). The new method also has the advantage that the identified "solar aperture" becomes physically interpretable. It can be seen as the equivalent mean solar transmission coefficient of the envelope (mainly the glazed components) under normal incidence, multiplied by the total glazed surface of the whole building envelope, and is denoted as $gA_{eq,tot,\perp}$ (replacing A_w in Eq. 12.1).

Both analyses have been done using 30 min sample time data, which has been found to be a good compromise between stability and aliasing for this type of modelling and other conditions mainly related to the building, the experiment and the weather.

State-of-the-Art Method Using Global South Vertical Solar Radiation Data

Using the "classic" approach, we obtained the results shown in Fig. 12.8.

The autocorrelation of the residuals is very close to white-noise but there is a clear signal left in the data from what can be seen in the cross-correlations between the main system variables and the residuals of the identification.

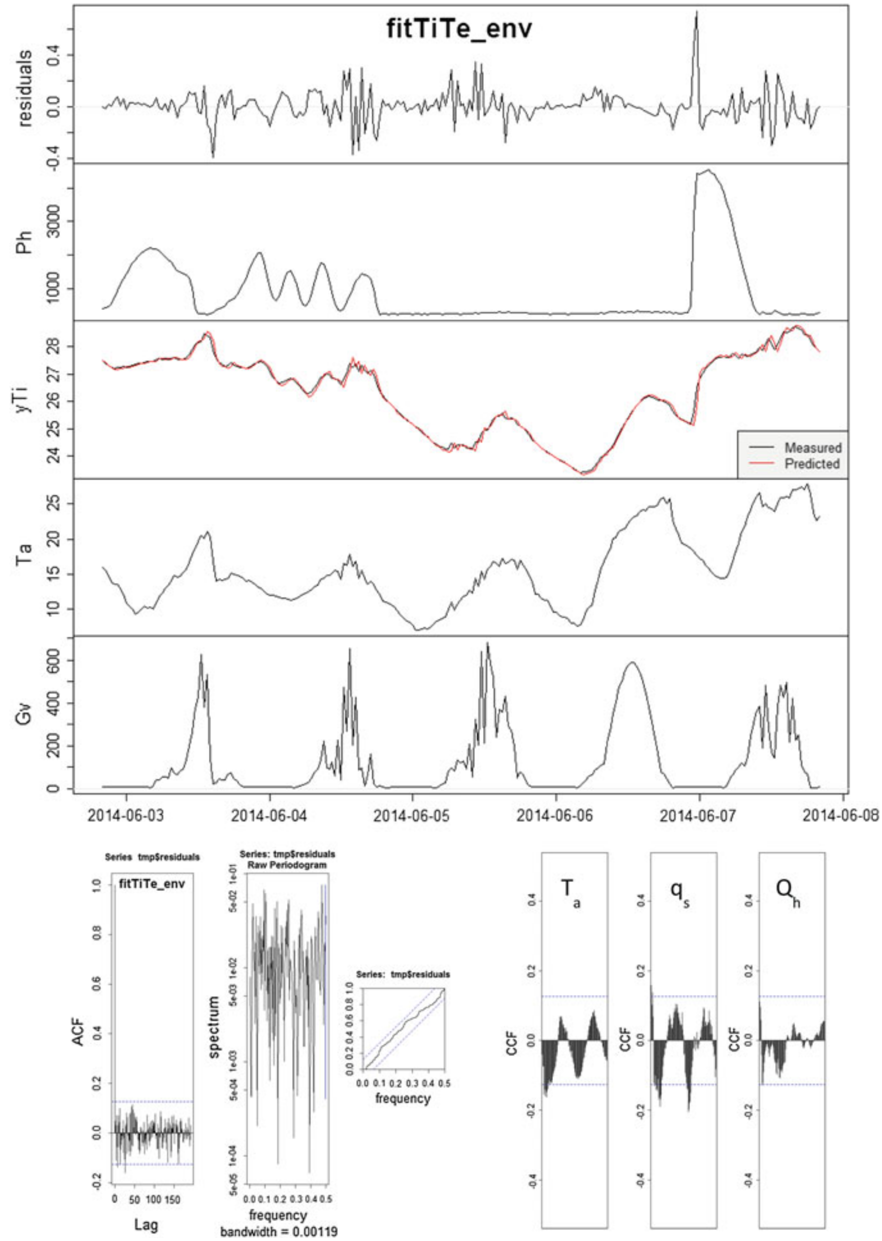

Fig. 12.8 On the *top* the residuals between the measured and predicted output of the model, the heating power, the inside and ambient air temperatures and *vertical south* solar radiation *bottom left* autocorrelation of the residuals, raw and cumulated periodograms (T_i) *bottom right* cross-correlations between the residuals and input variables (T_a, $q_{s,v,south}$, Q_h)

The identified UA-value is 143.25 ± 5.54 W/K. It has a confidence interval limited to 4 % which is very small. Note that the total heat losses were corrected with the exfiltration losses in the modelling, such that the result is expressed in terms of the UA-value instead of the HLC. Using the vertical south global solar radiation ($q_{s,v,south}$) as input, the identified solar aperture (A_w) is 5.4 ± 3.4 m^2. It has a confidence interval of 63 % which is very big. Moreover, intuitively, one could consider that the result is small compared to the total glazed surface of the building (23 m^2), and even of the glazed surface of the south façade only (15 m^2). Nevertheless, since the solar aperture does not have any physical interpretation, such an assessment is not allowed, and we only can state that the result carries a big uncertainty. This uncertainty very probably comes from the fact that the solar radiation that was used as input in the model is not a good explanatory variable of the evolution of the interior temperature and is not very suited for the kind of dynamic analysis we made.

We will see in Section "Analysis Results" that a bigger result is found. Nevertheless it is important not to simply compare the magnitude of both results, since the underlying definitions are different. In the newly proposed definition, the aperture is to be understood under normal radiation, which obviously better transmits the radiation than under global radiation composed of beam but not specifically normal and diffuse parts.

New Method Using Pre-processed Equivalent Normal Solar Radiation Data

Methodology for the Pre-processing of the Data

The methodology used in this paper has already been developed in (Lethé et al. 2013). The transmission through glazed components[3] is a non-linear decreasing function of the incidence angle (see norm EN 410 § 4.2). Moreover, the solar radiation is never a pure beam and the glazed components of the building are orientated (and possibly inclined) specifically for each façade. Therefore, we are aiming in this paper at identifying solar aperture coefficients that physically relate to distinct surfaces and under a normalized solar radiation. Under this definition of the solar aperture, we expect that results based on pre-processed inputs to be more replicable to various periods of the year and geographic climates too (it is expected that the same HLC is obtained for an exact same house built in various countries and monitored in different periods).

[3]We here neglect the transmission through opaque components since it is more than one order of magnitude lower for relatively highly glazed building envelopes, often encountered in some residential building sectors aiming at maximizing free solar gains. The reader can refer to (Gorse et al. 2014) and in the norm ISO 13792:2005 § 4.2.3 for more information.

The modified inputs for each façade are calculated as described below. A distinct treatment is applied to the beam and the diffuse parts of the solar radiation. In both cases, some approximations have been required.

First, a numerical model (CAPSOL, Physibel) is used to obtain the position of the sun in the sky (altitude and azimuth) at each time step. The ground albedo was assumed isotropic and stable, with a value of 0.2 (green grass surrounding the building). Based on the measured global and diffuse horizontal solar radiations, an anisotropic sky model (Muneer, embedded in CAPSOL) reproduces the direct and diffuse radiations for each façade. These have been found consistent with the direct measurements (especially for the highly glazed south façade). This process is time-consuming but useful if a lot of façades with different orientations are present, since only two measurements of solar radiation are required. Refinements in the modelling are required in case of surrounding buildings or obstacles to the solar radiation, which was not significant in our study.

Next, the angle of incidence (hereafter, AOI) between the beam radiation direction and each façade are computed, and a decreasing normalized function is evaluated to simulate the generic transmission behaviour of the glazing (see Fig. 12.9) and obtain the instantaneous reduction coefficients. This function is a simplification function from EN 410 § 4.2:

$$c = 1 - (\tan(AOI/2))^{2.5*2} \tag{12.7}$$

which correctly evaluates to 1 for a normal incidence and to 0 for a grazing angle of incidence.

In case the building is equipped with a mix of double and triple glazing, the choice of the tangent function exponent requires some optimisation. In our case, only double conventional glazing is present, and the proposed function is very close to the reference behaviour of these transparent components. More generally, this approximation is better than neglecting the angular effect in the transmission properties of glazing as done by default by most practitioners.

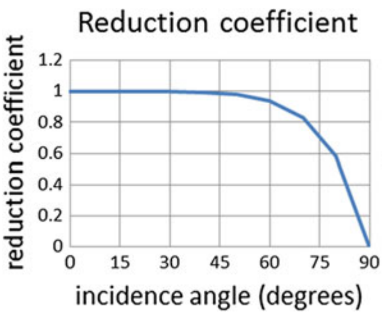

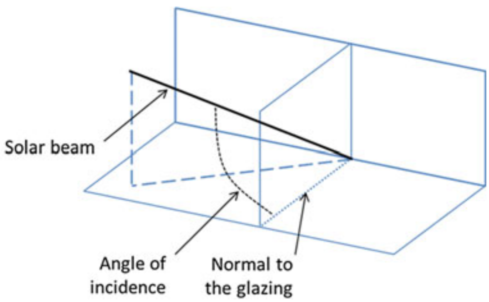

Fig. 12.9 Reduction coefficient for the transmission as a function of the AOI and the definition of the angle of incidence according to the norm EN 14500 § 3.3

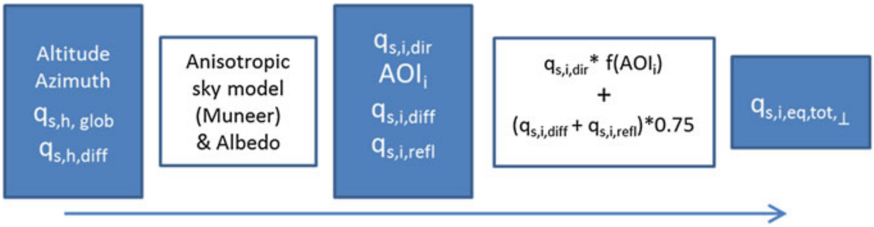

Fig. 12.10 Process to obtain the equivalent beam normal incidence total solar radiation on each façade

For the diffuse part of the solar radiation (both from the sky and reflected on the ground), previous experiences, e.g. with the WIS software (Window Information System), indicated that a reduction factor of 0.75 could be applied as a default approximation. Obtaining more accurate approximations is clearly out of the scope of this paper and probably too complex to be applied systematically.

Finally, the solar radiation terms are each multiplied with their reduction coefficients and summed to obtain the equivalent beam normal incidence total solar radiation ($q_{s,eq,tot,\perp}$) already mentioned in Section "Energy Balance of a Building Envelope", that is used as the input, and the parameter $gA_{eq,tot,\perp}$ can be identified.

The complete preparation process is represented in the Fig. 12.10, where the blue cells correspond to data and the white cells to computing steps. In this figure, $q_{s,h,\ glob}$ and $q_{s,h,diff}$ are the global and diffuse horizontal solar radiation, $q_{s,i,dir}$, $q_{s,i,diff}$, $q_{s,i,refl}$ are respectively the direct, diffuse and reflected solar radiation on the glazed components (of the façade) of index i and $q_{s,i,eq,tot,\perp}$ is the equivalent beam normal incidence solar radiation for the glazed components (of the façade) of index i.

Finally, to obtain the modified input to be applied to the building as a whole, we make a surface-weighted average for all the façades (the surfaces A_i are the surfaces of the glazed components):

$$\frac{\sum A_i q_{s,i,eq,tot,\perp}}{\sum A_i} \tag{12.8}$$

Implementation of the Pre-processing on the Full-Scale Hybrid Experiment

The full process explained in § 0 has been applied on the hybrid experiment data presented in Fig. 12.4.

Figure 12.11 shows the correspondence (ratio) between the crude and the modified solar radiation variables ($q_{s,v,south}$ and $q_{s,eq,tot,\perp}$). Globally, the modified input is about 56 % of the crude vertical south solar radiation. We nevertheless see that the ratio evolves during the day and that the daily pattern also depends on the type of sky. The pattern is especially time-varying during the fourth day which has

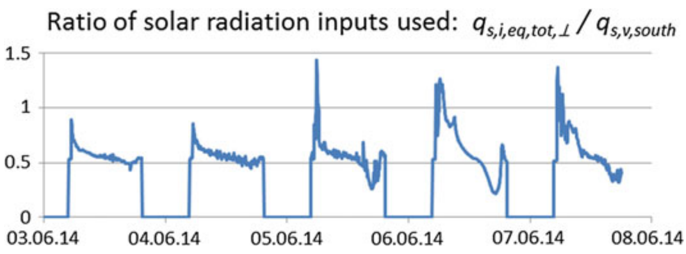

Fig. 12.11 Ratio between crude and modified solar radiation input

a clear sky (mostly beam radiation). For that reason, neither a static aperture coefficient nor a fixed daily curve should be applied if a highly accurate representation of the building system dynamic is desired.

Nevertheless, this observation should be tempered since known methods have shown that obtaining the steady-state Heat Loss Coefficient is possible without paying in-depth attention to the detailed modelling of solar gains. Contrarily, some methods concentrate the measurements at night when there is no solar radiation and some others try to minimize the solar gains using screens on the windows or closing the shutters.

Analysis Results

Using the new method, we obtained the results shown in Fig. 12.12.

The autocorrelation of the residuals is very close to white-noise and it also seems this time that very few specific cross-correlations remain between the system variables and the residuals of the identification, although the model still can be improved from what can be seen in the cumulated periodogram, for example, by a discretization of the building envelope with two serial capacities.

The identified UA-value is 144.4 ± 25 W/K. It has a much bigger confidence interval than in § 0 (17 % instead of 4 %) but the estimated centre value did not change significantly (>1 % difference).

Using the equivalent beam normal incidence total solar radiation ($q_{s,eq,tot,\perp}$) as input, the identified solar aperture ($gA_{eq,tot,\perp}$) is 18.8 ± 6.5 m^2. It has a confidence interval of 34 % which is still big but about half the value found previously (63 %). This time, we can compare the estimated centre value with the total glazed surface of the building (23 m^2). By making the ratio, we obtain an equivalent mean g-value of 0.82 which seems physically very reasonable compared to a solar factor of a conventional double glazing, and demonstrates the capability of the method to identify a physically-interpretable solar aperture.

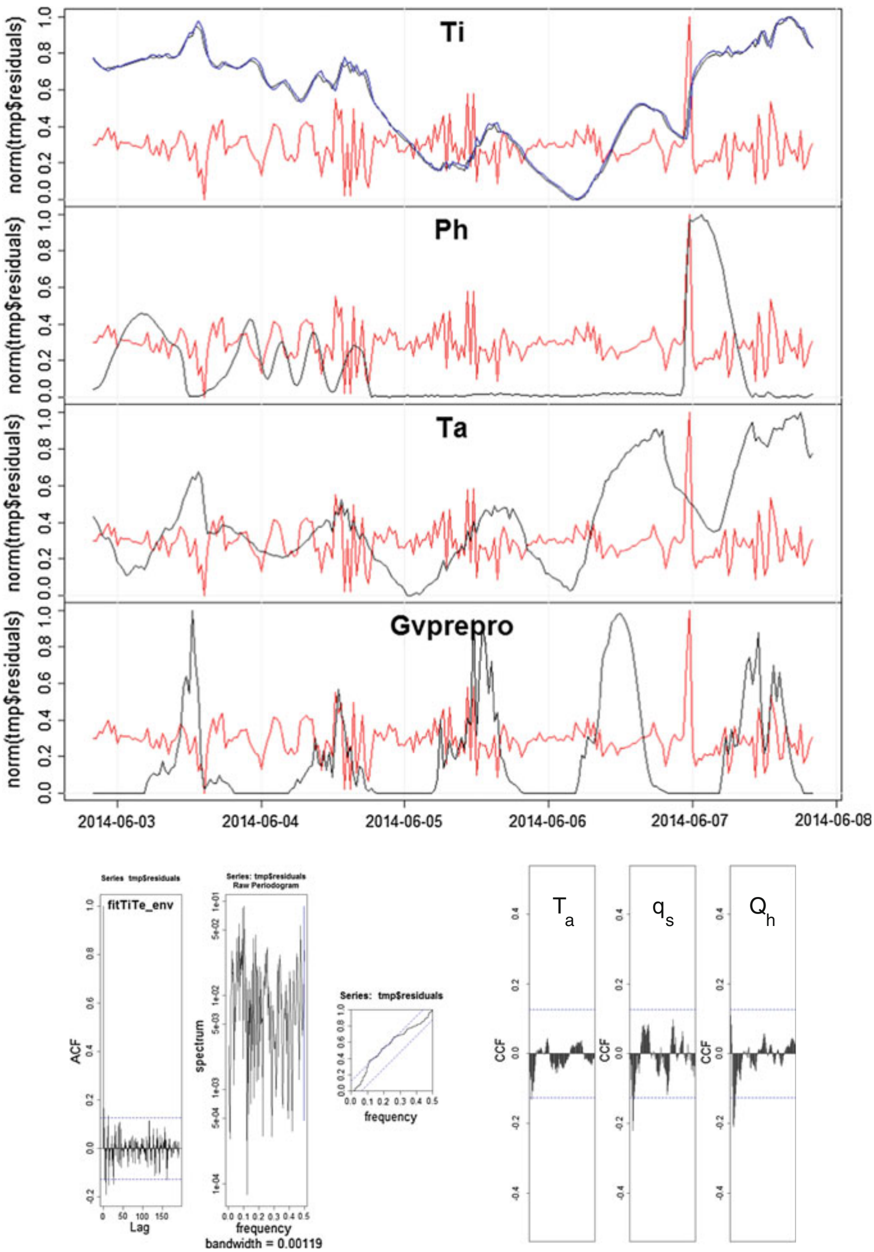

Fig. 12.12 On the *top* the residuals between the measured and predicted output of the model, the heating power, the inside and ambient air temperatures and *equivalent* solar radiation *bottom left* autocorrelation of the residuals, raw and cumulated periodograms (T_i) *bottom right* cross-correlations between the residuals and input variables (T_a, $q_{s,eq,tot,\perp}$, Q_h)

Comparison of the Approaches

We can also compare the order of magnitude of the two ‘solar aperture’ estimated values and the two solar radiation inputs. We saw that $q_{s,eq,tot,\perp}/q_{s,v,south}$ yielded a mean value of 0.56. Hence, computing the ratio $A_w/gA_{eq,tot,\perp}$ could be expected to yield a similar value. Nevertheless, it is only 0.29. This difference can of course be due to the non-linearities present in the physical problem, but might also reveal that the identified solar aperture A_w was underestimated. Though, in this case, it does not seem to have had a significant impact on the estimation of the UA-value, only slightly smaller than the UA-value obtained with the advanced method. Yet, it is probable that the second method is more accurate in a prediction or simulation context (required for example for model predictive control). Above all, it looks clear that the second method provides stronger results in terms of the solar aperture, which was the purpose of the study.

Looking now at the estimation of the UA-value, we also notice that the confidence interval has significantly increased when moving from the classic to the more detailed methodology. Additionally, the cumulated periodogram seems less optimal, even though the average of the residuals became slightly lower. It is not sure whether the log-likelihood criteria might be used in this context to compare both approaches, since the number of variables and parameters remain unchanged. These criteria respectively give 175 and 199 which is very similar anyhow. The reasons of that unexpected result are not well understood. We can argue that the quality indicators loose some consistency when measured data gets pre-processed, even though physical results and estimates make good sense. Maybe the pre-processing of the solar data impacted the optimisation space such that it became less convex for the UA-value, hence producing larger confidence bounds. Maybe the relatively high (and invariable) value assumed for the albedo could also explain such a pattern. A lower value (such as 0.15) would probably provide sharper results. These observations offer new challenges to the physical and statistical practitioners, although the obtained results are already very interesting and probably complex enough for large scale *in situ* applications.

Conclusions

To reliably determine the main parameters of a building model or building component requires that the test environment, but also the experimental procedure and data analysis are treated carefully. Then, the heat loss coefficient and more specifically the transmission losses can be estimated with various methods and for different purposes. The infrastructure and methodology developed in this paper showed the following advantages compared to existing ones:

– short dynamic testing (5 days) thanks to the optimisation of the decorrelation of the system variables making the test less expensive and more applicable to buildings that cannot be left empty for a longer period, required both for static co-heating tests (15 days) and conventional dynamic ones (10 days).
– control of the heating power injected to produce smooth data sets and hence facilitate the residual analysis and the results validation.
– adaptive multi-zone spread of the power injection to increase the temperature homogeneity inside the building, hence the accuracy of the aggregated indoor air temperature and eventually the temperature gradient with respect to the ambient temperature.
– higher accuracy of the identification of the solar aperture and its physical interpretation that allows a sanity-check of the result and better dynamic prediction models.

As a drawback to the latter point, compared to conventional techniques, the measured solar data needs to be pre-processed and the albedo and surrounding obstacles have to be modelled, or extra pyranometers have to be used to avoid this preparation work. Moreover, the surface and orientation of each glazed component must be known precisely enough.

Alternatively, measurements could be concentrated at night when there is no solar radiation or solar gains could be minimized using screens on the windows or closing the shutters. The resulting model is in this case less informative and is primarily aimed at extracting the static heat loss coefficient.

Another alternative to the 'nearly white-box' modelling presented in this study might be located closer to a 'nearly black-box' modelling: the solar aperture is then represented by a daily curve, encapsulating all the solar-related physical phenomena. Two distinct solar aperture curves are required for the beam and for the diffuse radiation to obtain good results, as was shown in Fig. 12.11. This should be further investigated.

Several other questions which were not extensively developed here and might be significant regarding:

– the correct estimation of the exfiltration losses for buildings that are not extremely airtight.
– other weather conditions such as the wind speed and orientation, and the sky temperature.
– the general treatment of adjacent spaces, heated or unheated and possible thermal by-passes.

The identification of informative and detailed models have several applications such as the estimation of the (steady-state or integrated) energy performance of the building, the prediction and control of the energy consumption and interior comfort, under specific weather forecasts (for model predictive control) or normalized weather conditions (for energy signature labelling).

Acknowledgments This paper is published in the context of the pre-normative research project 'PERFECT' with the financial support of the Belgian Bureau for Standardisation (NBN).

We hereby thank all the people involved in the measurements for their support and more specifically Brieuc Meurisse.

We thank the whole group of IEA Annex58 members and specially Peder Bacher, Geert Bauwens, Guillaume Pandraud and Pavel Kopecky for the interesting discussions and shared ideas during and between the expert meetings.

References

Bacher, P., & Delff, Ph. (2013). *Grey-box models for thermal performance characterization of a testbox.* Technical University of Denmark, IEA Annex 58—Subtask 3—CE 4.

Bacher, P., & Madsen, H. (2011). Identifying suitable models for the heat dynamics of building. *Energy and Buildings, 43*, 1511–1522.

Bacher, P., Thavlov, A., & Madsen, H. (2010). *Models for energy performance analysis: financed by the Danish electricity saving trust.* Technical University of Denmark, DTU Informatics, IMM-Technical Report Feb 2010.

Bauwens, G., & Roels, S. (2014). Co-heating test: a state-of-the-art. *Energy and Buildings, 82*, 136–172.

Gorse, C., et al. (2014). *The gap between calculated and real performance: experiences from the field and the measures required to address the difference*. CeBE: Leeds Sustainability Institute.

ISO, 9869-1. (2014). Thermal insulation—Building elements—*In-situ* measurement of thermal resistance and thermal transmittance—Part 1: Heat flow meter method. 1st edition.

Johnston, D., Miles-Shenton, D., Farmer, D., & Wingfield, J. (2013). *In-situ thermal performance of construction products, building elements and structures.* N0191 whole house heat loss test method (Co-heating). CEN/TC 89/WG 13.

Lethé, G., et al. (2013). *Dynamic analysis replication of a testbox in various climates*. Belgian Building Research Institute, IEA Annex 58—Subtask 3—CE 4.

Lethé, G., et al. (2014). *An adapted co-heating test and experimental infrastructure for thermal dynamic response and performance identification of residential buildings*. In: 9th international conference on system simulation in buildings.

Pandraud, G., Mangematin, E., Roux, D ., & Quentin, E. (2013). *QUB: a new rapid building energy diagnosis method.* In 11th REHVA world congress and 8th international conference on IAQVEC.

Steskens, P., Lethé, G., & Flamant, G. (2014). *The application of a modified co-heating test and grey-box modelling for predicting building thermal dynamics*. In 10th Nordic symposium on building physics. Lund, Sweden. 15–19 June 2014.

Subbarao, K., et al. (1988). *Short-Term Energy Monitoring (STEM): Application of the PSTAR Method to a Residence in Fredericksburg, Virginia.* Solar Energy Research Institute, US Department of Energy, Task No. SB811241.